BAF-1 mobility is regulated by environmental stresses

Daniel Z. Bar[a,*], Maya Davidovich[a,*], Ayelet T. Lamm[a], Hagit Zer[a], Katherine L. Wilson[b], and Yosef Gruenbaum[a]

[a]Department of Genetics, Institute of Life Sciences, Hebrew University of Jerusalem, Givat Ram Jerusalem 91904, Israel; [b]Department of Cell Biology, Johns Hopkins University School of Medicine, Baltimore, MD 21205

ABSTRACT **Barrier to autointegration factor (BAF) is an essential component of the nuclear lamina that binds lamins, LEM-domain proteins, histones, and DNA. Under normal conditions, BAF protein is highly mobile when assayed by fluorescence recovery after photobleaching and fluorescence loss in photobleaching. We report that *Caenorhabditis elegans* BAF-1 mobility is regulated by caloric restriction, food deprivation, and heat shock. This was not a general response of chromatin-associated proteins, as food deprivation did not affect the mobility of heterochromatin protein HPL-1 or HPL-2. Heat shock also increased the level of BAF-1 Ser-4 phosphorylation. By using missense mutations that affect BAF-1 binding to different partners we find that, overall, the ability of BAF-1 mutants to be immobilized by heat shock in intestinal cells correlated with normal or increased affinity for emerin in vitro. These results show BAF-1 localization and mobility at the nuclear lamina are regulated by stress and unexpectedly reveal BAF-1 immobilization as a specific response to caloric restriction in *C. elegans* intestinal cells.**

Monitoring Editor
Thomas M. Magin
University of Leipzig

Received: Aug 19, 2013
Revised: Jan 21, 2014
Accepted: Jan 24, 2014

INTRODUCTION

Barrier to autointegration factor (BAF) is an essential, 10-kDa protein expressed in multicellular animals (Zheng *et al.*, 2000; Furukawa *et al.*, 2003; Margalit *et al.*, 2005b). BAF was first identified as a mammalian protein required for retroviral DNA to integrate into the host chromosome (Chen and Engelman, 1998) and is required for human immunodeficiency virus 1 integration into macrophage chromosomes (Lin and Engelman, 2003; Jacque and Stevenson, 2006; Shun *et al.*, 2007; Van Maele *et al.*, 2006). BAF was independently identified as a novel partner for the nuclear membrane protein lamina-associated polypeptide 2β (LAP2β, encoded by *TMPO*; Furukawa, 1999) and subsequently shown to bind the LAP2, emerin, MAN1 (LEM) domain of LAP2 (Shumaker *et al.*, 2001), which is shared by all members of the LEM-domain family of nuclear proteins (Shumaker *et al.*, 2001; Margalit *et al.*, 2007a).

Homodimers of BAF bind nonspecifically to double-stranded DNA (Cai *et al.*, 1998; Zheng *et al.*, 2000), allowing it to "bridge" two DNA molecules in vitro (Bradley *et al.*, 2005) or "condense" longer DNA molecules in vitro by making loops (Skoko *et al.*, 2009). BAF also directly binds three fundamental groups of proteins: LEM-domain proteins (Cai *et al.*, 2001, 2007; Lee *et al.*, 2001; Wagner and Krohne, 2007), histones (H3, H4, and certain H1 isoforms; Montes de Oca *et al.*, 2005, 2009), and nuclear intermediate filament proteins, named lamins (Lee *et al.*, 2001). BAF, lamins, and LEM-domain proteins can bind each other directly and simultaneously (Holaska *et al.*, 2003) and potentially synergistically (Bengtsson and Wilson, 2006). In *Caenorhabditis elegans*, all three components are required to assemble the nuclear "lamina" (Liu *et al.*, 2003; Margalit *et al.*, 2005b; Simon and Wilson, 2011), a major component of nuclear structure (Simon and Wilson, 2011).

Biochemical studies of BAF are challenged by its poorly understood ability to oligomerize as hexamers of dimers in the presence of DNA (Skoko *et al.*, 2009). Excess BAF profoundly disrupts higher-order chromatin structure in cell extracts (Segura-Totten *et al.*, 2002).

This article was published online ahead of print in MBoC in Press (http://www.molbiolcell.org/cgi/doi/10.1091/mbc.E13-08-0477) on February 5, 2014.

*These authors contributed equally to this article.

Address correspondence to: Yosef Gruenbaum (gru@vms.huji.ac.il).

Abbreviations used: BAF, barrier to autointegration factor; FLIP, fluorescence loss in photobleaching; FRAP, fluorescence recovery after photobleaching; GFP, green fluorescent protein; HPL-1/HPL-2, heterochromatin protein 1; LAP2β, lamina-associated polypeptide 2β; LEM domain, LAP2, emerin, MAN1 domain; LEM-4L, LEM-4–like; MBP, maltose-binding protein; PP2A, protein phosphatase 2A; RNAi, RNA interference; RU, resonance units; VRK1, vaccinia-related kinase 1.

In living cells, BAF influences higher-order chromatin structure (Furukawa *et al.*, 2003; Margalit *et al.*, 2005a; Haraguchi *et al.*, 2007), represses transcription at specific promoters (Wang *et al.*, 2002; Margalit *et al.*, 2007b; Huang *et al.*, 2011), and is required for post-mitotic nuclear assembly (Margalit *et al.*, 2005a). Through mechanisms that are not understood, BAF helps tether chromatin to the nuclear envelope (Margalit *et al.*, 2005a; Asencio *et al.*, 2012) and functions as an epigenetic regulator (Montes de Oca *et al.*, 2011). Depletion of BAF-1 dramatically increases susceptibility to radiation in *C. elegans* (Dittrich *et al.*, 2012).

In living cells, the DNA-binding activity of BAF and its nucleocytoplasmic distribution are controlled by a conserved Ser/Thr kinase named vaccinia-related kinase 1 (VRK1; Nichols *et al.*, 2006; Gorjánácz *et al.*, 2007). The distribution of BAF can change dramatically during the cell cycle (Dechat *et al.*, 2004; Haraguchi *et al.*, 2007; Capanni *et al.*, 2010; Asencio *et al.*, 2012). VRK1 phosphorylates human BAF residues Thr-2, Thr-3, and Ser-4 (Nichols *et al.*, 2006). Phosphorylation at Ser-4 reduces binding to emerin and abolishes DNA binding, whereas phosphorylation at Thr-2 or Thr-3 reduces binding to DNA (Bengtsson and Wilson, 2006; Nichols *et al.*, 2006). In *C. elegans*, BAF-1 can be dephosphorylated either directly, by protein phosphatase 2A (PP2A, mediated by cobinding to LEM-4–like [LEM-4L]), or passively, via LEM-4L–dependent inhibition of VRK-1 (Asencio *et al.*, 2012).

Previous FLIP/FRAP studies of green fluorescent protein (GFP)-fused lamin A, lamin B, emerin, LAP2β, and MAN1 showed these nuclear lamina components are predominantly immobile. The immobile fractions of lamin A and lamin B2 are ~95%, and similar $t_{1/2}$ recovery times were measured for lamin A (87 ± 25 s), lamin B1 (120 ± 40 s), emerin (62 ± 31 s), and MAN1 (97 ± 64 s) (Moir *et al.*, 2000; Shimi *et al.*, 2004; Broers *et al.*, 2005; Schutz *et al.*, 2005). By contrast, most GFP::BAF is mobile in both interphase human cells ($t_{1/2}$ of 270 ± 49 ms at the nuclear periphery, ~80 ms in the nucleoplasm, and ~47 ms in the cytoplasm; Shimi *et al.*, 2004) and in *C. elegans* embryos (2.24 ± 0.66 s; Margalit *et al.*, 2007b). This mobility suggested BAF-1 might function as a mobile "communicator" component of the nuclear lamina. We tested this hypothesis by fluorescence loss in photobleaching (FLIP) and fluorescence recovery after photobleaching (FRAP) analysis of *C. elegans* lines bearing integrated wild-type or missense-mutated GFP::BAF-1. We report GFP-BAF-1 is immobilized in L1 larvae subjected to dietary restriction (*eat-2* mutant), food deprivation, or brief (1 h) heat shock.

RESULTS

We previously showed that an integrated GFP::BAF-1 construct rescues most known *baf-1* null (*gk324*) phenotypes (Margalit *et al.*, 2007b). To determine whether BAF-1 mobility was affected by stress, we used FRAP to analyze GFP::BAF-1 localization and dynamics in cells of L1 and L2 larval of wild-type (N2) or *eat-2* animals. The *eat-2* mutation disrupts a ligand-gated ion channel, resulting in decreased pharyngeal contractions and dietary restriction (Mastick *et al.*, 1995). Photobleached regions recovered rapidly in both the wild-type and *eat-2* animals; however, a significantly ($p < 0.01$, two-tailed *t* test) higher fraction of GFP::BAF-1 was immobile in the *eat-2* animals (Figure 1A). To determine whether this phenotype was specifically due to starvation or another effect of the *eat-2* mutation, we studied wild-type animals that were either fed or food-deprived overnight. The next day, fed animals had reached the L1 or L2 larval stage, whereas food-deprived animals were exclusively in L1, as previously reported (Johnson *et al.*, 1984). Consistent with the *eat-2* results, FRAP analysis revealed an increase in the immobile fraction of GFP::BAF-1 in food-deprived animals (Figure 1B). This difference

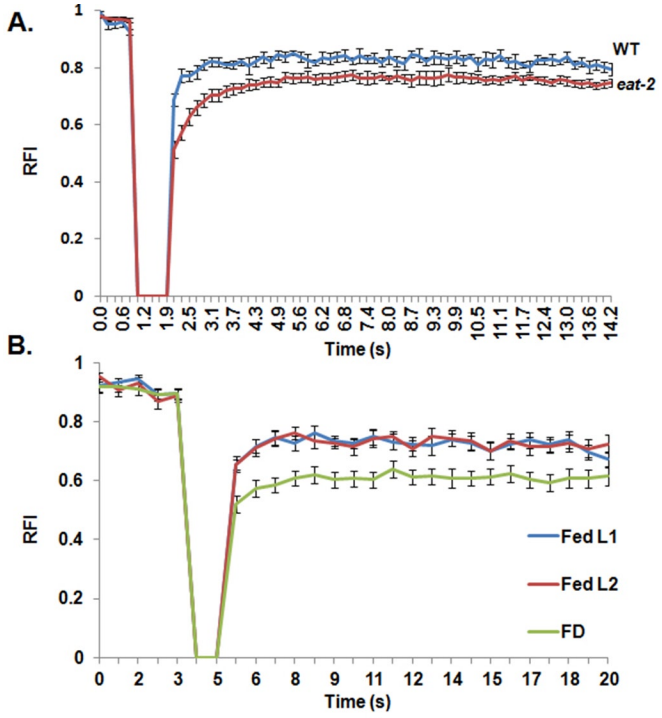

FIGURE 1: *Eat-2* mutation and food deprivation reduce the mobile fraction of GFP::BAF-1 in L1 larvae. (A) FRAP analysis of GFP::BAF-1 in wild-type (blue) or in *eat-2* (ad1116; red) *C. elegans* L1 larvae. $n = 7$ and 12, respectively. (B) FRAP analysis of GFP::BAF-1 in wild-type L1 (blue), wild-type L2 (red), or food-deprived (FD) L1 (green) animals. Error bars indicate SEM. *x*-axis: time; *y*-axis: relative fluorescence intensity (RFI). $n = 15$, 15, and 30 for L1, L2, and FD, respectively. Bleaching area: 2.8 μm^2.

was significant ($p < 0.00056$, two-tailed *t* test) and did not depend on larval stage, as L1 and L2 well-fed controls gave the same results (Figure 1B).

Because intestinal cells have major roles in responding to food deprivation (Walker *et al.*, 2005; Palgunow *et al.*, 2012), we focused on intestinal cell nuclei of L1- and L2-stage wild-type (N2), *eat-2*, and food-deprived animals. As BAF-1 is highly mobile, the bleaching in FRAP must be short, which reduces bleach depth. To overcome this technical problem, we used FLIP analysis to more accurately measure the immobile fraction and obtain a better quantitative representation of the phenomena (Figure 2). We bleached a small region overlapping the nucleus for ~1 min, while observing the whole cell. In wild-type animals, this caused an almost complete disappearance of GFP::BAF-1 fluorescence at the nuclear envelope and throughout the cell (Figure 2, A–C, wild-type/fed), as expected (Margalit *et al.*, 2007b). By contrast, in both the *eat-2* and food-deprived intestinal cells, GFP::BAF-1 fluorescence outside the bleached area was essentially unaffected (FD animal cells shown in Figure 2A and GFP::BAF-1 in fed and food-deprived intestinal cells shown in Supplemental Movies S1 and S2, respectively). This suggested that nearly all GFP::BAF-1, notably including the nuclear lamina population, was immobilized in response to dietary stress. There was no correlation between GFP::BAF-1 fluorescence intensity, which can vary between different intestinal cells, and its mobility. Immobilization was only slowly reversible, as food-deprived animals that were returned to feeding plates for 2 h ("FD/fed") showed a slight but significant increase in GFP::BAF-1 mobility (Figure 2C; $p < 0.05$, $n = 6$, two-tailed *t* test). Thus BAF immobilization may be a relatively

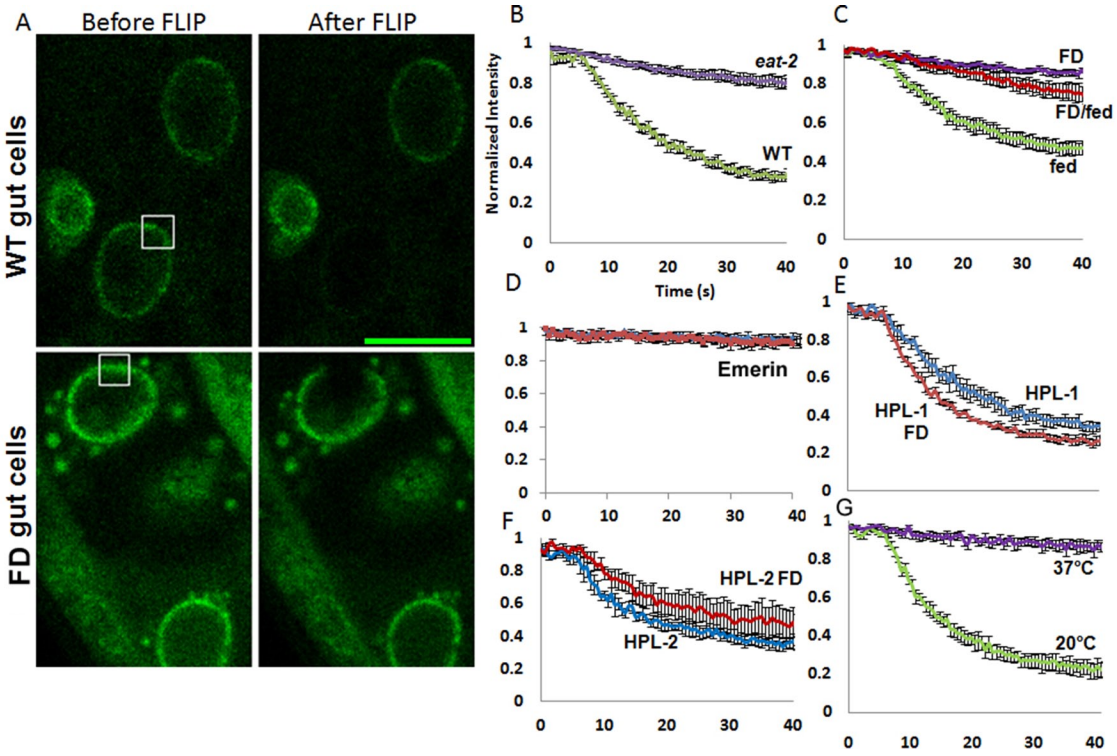

FIGURE 2: FLIP analysis of intestinal cells in L1 larvae reveals reduced GFP::BAF-1 mobility in response to dietary restriction, food deprivation, or 1-h heat shock. (A) FLIP analysis of GFP::BAF-1 in intestinal cells of L1 larvae in wild-type (top) or in *eat-2* animals (bottom). Scale bar: 5 µm. (B) Mobility plot of the relative intensity of the GFP::BAF-1 in wild-type (green line) and *eat-2* animals (purple). (C) Mobility plot of the relative intensity of the GFP::BAF-1 in *C. elegans* L1 larvae that were well fed (blue line), animals that were food deprived overnight (red line), or following 2-h recovery from FD (green line). FLIP analysis of emerin (D) HPL-1 (E) and HPL-2 (F) fused to GFP did not reveal any difference in mobility after food deprivation. (G) Mobility plot of the relative intensity of GFP::BAF-1 in wild-type animals with time following 1-h heat shock at 37°C. Error bars indicate SEM. For each experiment in (B), $n = 7$; in (C–G), $n = 6$. *x*-axis: time; *y*-axis: relative fluorescence intensity (RFI). The nuclei shown here were taken from the anterior part of the intestine. Bleaching area: 2 µm^2.

long-term response to dietary stress in intestinal cells (see *Discussion*).

To determine whether other chromatin- or lamina-associated proteins were immobilized by food deprivation, we used FLIP to measure the mobility of GFP-fused heterochromatin protein 1 (HPL-1 and HPL-2; Schott *et al.*, 2006) or emerin in intestinal cells. Food deprivation had no significant affect on the mobility of these proteins (Figure 2, D–F). Thus wholesale immobilization is not a general phenomenon of chromatin-associated proteins.

Short heat shock is known to extend life span, potentially by activating small heat shock proteins and other stress-response genes (Olsen *et al.*, 2006). Interestingly, a brief heat shock (1 h at 37°C) also significantly reduced GFP::BAF-1 mobility in the intestine (Figure 2G) and in epidermal and muscle cells of wild-type L1 or L2 animals (Supplemental Figure S1A and unpublished data). These results are stage specific, as adult worms showed weaker GFP::BAF-1 immobilization in response to heat shock, and early-stage embryos showed an inverse response (Figure S2). As BAF-1 is an essential protein, we knocked down *baf-1* postdevelopmentally and tested heat shock survival. Despite the role of heat shock in BAF-1 mobility, we saw no effect of *baf-1* RNA interference (RNAi) on animal survival (12 h at 35°C; unpublished data). However, we cannot exclude an essential role for *baf-1* in other stresses or developmental stages. These results collectively showed that GFP::BAF-1 is specifically immobilized at the nuclear envelope and elsewhere in response to three different cellular stresses: dietary restriction (*eat-2*), food deprivation, and brief heat shock. To explore the mechanisms by which food deprivation and stress pathways regulate BAF-1 dynamics, we focused on heat shock, which triggers some of the same signaling pathways as food deprivation (Raynes *et al.*, 2012), affects BAF-1 mobility in most or all cell types, and is readily manipulated in adult animals.

GFP-BAF-1 Ser-4 phosphorylation doubles in response to short heat shock

To determine whether BAF-1 was posttranslationally modified in response to stress, we immunoprecipitated GFP::BAF-1 from unsynchronized populations of control or heat-shocked (1 h, 37°C) mixed population *C. elegans* (Rothbauer *et al.*, 2008) and used mass spectrometry to detect posttranslational modifications. GFP::BAF-1 resolved as two abundant bands (Figure S3), similar to endogenous human BAF (Puente *et al.*, 2011), in which the slow-migrating BAF band is proposed to be hyperphosphorylated (Nichols *et al.*, 2006). Both bands were analyzed by liquid chromatography–tandem mass spectrometry, with tryptic peptide coverage of ~80% (Figure 3A). We detected the same modification in all four bands: phosphorylation at Ser-4 (Figure 3A). No other phosphorylated residues were detected. For each sample, the relative amount of the Ser-4–phosphorylated peptide, CAAGPGSTGMSTSVK, was estimated as a fraction of the intensity (total ion current) of its corresponding

A

Peptide sequence	Control		Heat Shock	
	Upper band	Lower band	Upper band	Lower band
CAAGPGSTGMSTSVK	Yes	Yes	Yes	Yes
GPGSTGMSTSVKHR	No	No	No	Yes
HREFVGEPMGDKEVTCIAGIGPTYGTK	No	No	No	Yes
EFVGEPMGDK	Yes	Yes	No	Yes
EFVGEPMGDKEVT	No	Yes	No	Yes
EFVGEPMGDKEVTCIA	No	No	No	Yes
EFVGEPMGDKEVTCIAGIGPTYGTK	Yes	Yes	Yes	Yes
EVTCIAGIGPTYGTK	Yes	Yes	Yes	Yes
LTDAGFDKAYVLFGQYLLLK	No	Yes	No	No
TDAGFDK	Yes	Yes	Yes	Yes
TDAGFDKAYVLFGQYLLLK	No	Yes	No	Yes
AYVLFGQYLLLK	Yes	Yes	Yes	Yes
KDEDLFIEWLK	Yes	Yes	Yes	Yes
KDEDLFIEWLKETAGVTANHAK	No	Yes	No	No
ETAGVTANHAK	No	Yes	No	Yes

B

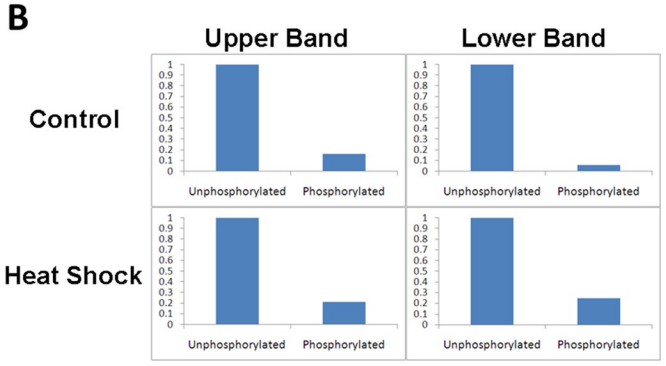

FIGURE 3: Mass spectrometry analysis of GFP::BAF-1 Ser-4 phosphorylation before and after heat shock of asynchronous *C. elegans* populations. (A) BAF-1 peptides identified by mass spectrometry. The overall peptide coverage was 80 and 82% from control and heat shock samples, respectively. (B) Relative intensity of mass spectrometry spectra showing the Ser-4–phosphorylated and nonphosphorylated BAF-1 peptide CAAGPGSTGMSTSVK from control animals (top) and heat-shocked animals (bottom).

nonphosphorylated peak (Figure 3B). In control animals, this Ser-4–phosphorylated peptide was more abundant in the upper band than in the lower band (Figure 3B). Because the upper and lower bands each comprised about half of the GFP::BAF-1, we concluded that GFP::BAF-1 Ser-4 phosphorylation increases in response to heat shock. This result was puzzling, as this modification on human BAF reduces binding to DNA and nuclear lamina proteins—seemingly in opposition to the immobilization phenotype.

Effects of BAF-1 missense mutations on GFP::BAF-1 localization in vivo

As controls to determine whether mutations at Ser-4 or elsewhere affected GFP::BAF-1 localization in *C. elegans*, we generated GFP::BAF-1 strains bearing each of four missense mutations: S4A (blocks modification at this position; weakens human BAF binding to lamin A, reduces binding to DNA, and modestly reduces binding to the LEM-domain; Bengtsson and Wilson, 2006; Nichols *et al.*, 2006), S4E (mimics phosphorylation; disrupts human BAF binding to lamin A; Bengtsson and Wilson, 2006), K6A (disrupts human BAF binding to DNA and histones; Harris and Engelman, 2000), and F46E (corresponding human L46E mutation disrupts binding to DNA, histones, and emerin; Segura-Totten *et al.*, 2002) (Figure 4A and Supplemental Table S1). To compensate for random integration and variation in expression level, we used each construct to generate at least two independent strains. All strains of the same construct had similar BAF-1 expression levels and expression patterns; one strain of each mutant was chosen for further studies.

Wild-type GFP::BAF-1 concentrated at the nuclear envelope in L1 larvae intestinal cells, with weaker signals in the nucleoplasm and cytoplasm, as expected (Figure 4B; Margalit *et al.*, 2005a). For comparison with each GFP::BAF mutant, we measured the GFP fluorescence intensity distribution across the nucleus in five to seven intestinal cells and then normalized and averaged by aligning the nuclear envelope peaks (trace below each image; Figure 4B). The S4A, S4E, and K6A polypeptides all concentrated near the nuclear envelope, like wild-type (Figure 4B). The F46E mutant also concentrated near the nuclear envelope but had higher signals in the nucleoplasm (Figure 4B). Thus three mutations did not visibly perturb GFP::BAF-1 localization in L1 larvae intestinal cells.

Effects of BAF-1 missense mutations on binding to lamin and emerin in vitro

With one exception, Ser-4 (Bengtsson and Wilson, 2006), the effects of BAF missense mutations on binding to lamins were unstudied. To determine whether our BAF-1 mutations affected direct binding to *C. elegans* partners, we generated recombinant maltose-binding protein (MBP) fusions to the N-terminus of wild-type or mutant BAF-1 and tested binding to three recombinant purified *C. elegans* proteins: emerin residues 1–125 (nucleoplasmic domain only), the lamin tail domain (residues 388–566), and full-length lamin bearing the R55H mutation (lamin-R55H) to maintain solubility when expressed in bacteria (Wiesel *et al.*, 2008). BIAcore surface plasmon resonance was used to measure association and dissociation constants and equilibrium affinities for BAF-1 binding to emerin (Figure 4C) or lamin-R55H (Figure 4D). Wild-type BAF-1 bound with high affinity to emerin (57 nM; reported affinity of human proteins is 200 nM; Holaska *et al.*, 2003). This variation may be species specific or may reflect differences in polypeptide constructs and assay conditions. Wild-type BAF-1 also bound with high affinity to lamin-R55H (84 nM; human BAF affinity for B-type lamins is untested). *C. elegans* lamin-R55H and emerin bound each other with 4–5 nM affinity (Figure 4C), 10-fold higher than that reported for human emerin and lamin A (40 nM; Holaska *et al.*, 2003); human emerin affinity for B-type lamins is untested). Emerin bound itself tightly (14 nM affinity; Figure 4C), consistent with human emerin (Berk *et al.*, personal communication). Full-length lamin (lamin-R55H) also showed high affinity for itself (3.7 nM) and to the isolated lamin tail domain (0.56 nM; Figure 4), suggesting that the lamin tail domain might mediate lateral association between lamin filaments in *C. elegans*.

All four tested BAF-1 mutations bound emerin with either wild-type affinity (~57 nM, S4E), two- to threefold higher affinity (31 nM, K6A; 20 nM, S4A), or 10-fold higher affinity (5.6 nM, F46E; Figure 4C). Note that the corresponding mutation in human BAF, L46E, abolished binding to human emerin in vitro (Segura-Totten *et al.*, 2002); whether this reflects a species-specific difference or extends to living cells (in which association can be influenced by other factors (e.g., posttranslational modifications) remains undetermined.

All four BAF-1 mutations reduced binding to full-length lamin R55H by either two- to threefold (K6A and S4A: 198 and 281 nM, respectively), seven- to ninefold (F46E, 623 nM), or 382-fold (S4E, 32.1 μM) (Figure 4D). Thus BAF-1 Ser-4 phosphorylation in *C. elegans* is predicted to inhibit binding to lamin without affecting emerin (see *Discussion*).

Heat shock–induced immobilization of GFP::BAF-1 in larvae intestinal cells is disrupted by the S4A and S4E mutations

To determine how BAF-1 mutations affected mobility, we used FRAP to analyze the GFP::BAF-1 mutants that localized normally in L1 larvae (K6A, S4E, S4A) both before and after 1-h heat shock (Figure 5A). We then calculated the percentage of each population that was mobile before, and immediately after, heat shock (Figure 5B). In L1 intestinal cells expressing wild-type GFP::BAF-1, mobility was

A

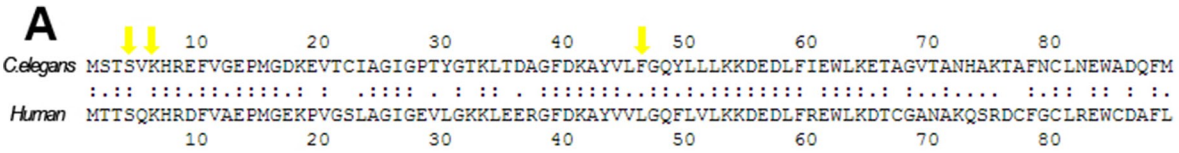

B

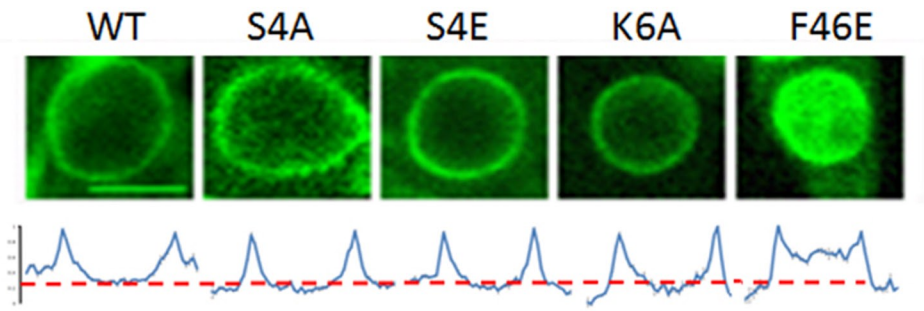

C

Bait: Emerin 1-125	Association constant	Dissociation constant	Affinity	χ^2
BAF WT	6.54E+4	2.91E-3	57.3 nM	1.96
BAF S4A	5.76E+4	6.24E-3	20.2 nM	1.6
BAF S4E	2.83E+4	1.66E-3	57.3 nM	2
BAF K6A	3.47E+4	8.74E-4	30.9 nM	1.89
BAF F46E	2.43E+5	1.38E-3	5.66 nM	1.72
Emerin 1-125	1.05E+5	1.48E-3	14.1 nM	0.535
Lamin Tail	1.17E+5	5.69E-4	4.07 nM	2.32
Lamin R55H	2.08E+5	1.08E-3	5.21 nM	1.93

D

Bait: Lamin R55H	Association constant	Dissociation constant	Affinity	χ^2
BAF WT	3.94E+4	3.3E-3	83.8 nM	2.2
BAF S4A	1.03E+4	2.89E-3	281 nM	1.42
BAF S4E	1.57E+2	5.04E-3	32.1 µM	2
BAF K6A	1.46E+4	1.79E-3	198 nM	0.808
BAF F46E	2.33E+5	1.45E-3	623 nM	1.93
Emerin 1-125	6.94E+4	1.91E-3	27.6 nM	0.379
Lamin Tail	8.95E+5	5.06E-4	0.56 nM	1.01
Lamin R55H	5.15E+5	1.89E-3	3.67 nM	2.34

FIGURE 4: In vivo analysis of wild-type and missense-mutant GFP::BAF-1 polypeptides. (A) Aligned amino acid sequences of BAF-1 (top) and human BAF (bottom), showing the missense mutations studied in this work (yellow arrow). (B) Fluorescence localization of GFP::BAF-1 (wild-type or mutant) protein in intestinal cell nuclei of L1 larvae. Scale bar: 5 µm. Each strain expresses a different GFP::BAF-1–based construct. The graph below each image shows the average intensity distribution across six nuclei (blue) on the same baseline as wild-type GFP::BAF-1 (red). (C and D) BIAcore analysis of the kinetics and equilibrium affinities of recombinant MBP::BAF-1, Ce-emerin residues 1–125, or Ce-lamin tail domain residues 388–566, each tested for binding to immobilized recombinant Ce-emerin residues 1–125 (C) or Ce-lamin R55H (D). χ^2 represents the mean square of the signal noise.

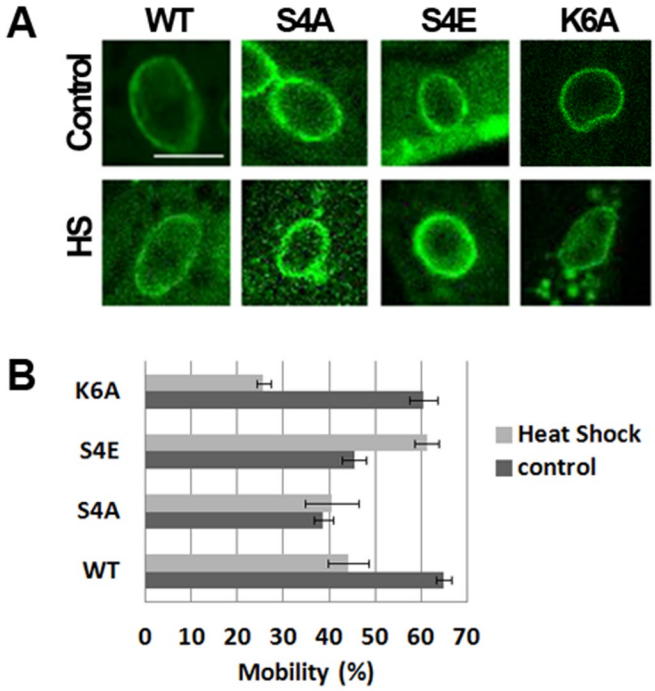

FIGURE 5: BAF-1 mobility in L1 larvae is affected by combined heat shock and S4A-, S4E-, and K6A-mutated GFP::BAF-1. FRAP analysis of larvae L1 intestinal cells expressing GFP::BAF-1 wild-type and mutant GFP-BAF-1 before and after heat shock (1 h, 37°C). (A) Images of L1 larvae with no heat shock (control, top) or after 1 h heat shock (bottom). Results graphed in (B) as the mobile percentage before and after heat shock in L1 larvae intestinal cells. Error bars indicate SEM. Scale bar: 5 μm. $n = 5–15$ for each data point.

reduced by heat shock as expected (from ~65% mobile to ~44%; Figure 5B and Table 1). The K6A mutant showed normal mobility before heat shock (~60%) but was hyperimmobilized by heat shock (25.7% mobile; Figure 5B and Table 1). The S4A mutant had reduced mobility (~39%) that was unaffected by heat shock (~40%; Figure 5B and Table 1). The S4E mutant had initially reduced mobility (~45%) and was hypermobilized by heat shock (~61%; Figure 5B and Table 1). Note that S4E affected BAF-1 mobility (45% mobile) at 20°C to the same extent as heat shock affected wild-type BAF-1 (44% mobile; Figure 5B and Table 1). To further validate the role of S4 phosphorylation in GFP::BAF-1 mobility, we down-regulated *vrk-1*, the BAF-1 kinase. Indeed, following *vrk-1* RNAi and heat shock, GFP::BAF-1 remained mobile, as compared with empty vector (Figure 6). These results mimic the phenotype of GFP::BAF-1 S4E, and support the role of phosphorylation in BAF-1 mobility. These results also support the hypothesis that BAF-1 mobility is regulated in intestinal cells by mechanisms that include (but are not limited to) posttranslational modification of Ser-4 and binding to emerin.

DISCUSSION

Under normal conditions, most nuclear BAF-1 is highly mobile during interphase, suggesting frequent but transient interactions (Shimi *et al.*, 2004; Margalit *et al.*, 2007b). Our FRAP and FLIP analyses of interphase cells showed GFP::BAF-1 becomes immobilized under multiple stress conditions. When larval-stage animals were calorie restricted through food deprivation or the *eat-2* mutation, BAF-1 was specifically immobilized in intestinal cells, with normal or intermediate phenotypes in other tested cell types, including muscle and epidermis (Figure S1B and unpublished data). By contrast, brief heat stress immobilized BAF-1 in all cell types tested, including intestinal, muscle, hypodermis, and pharyngeal cells (unpublished data). Immobilization was not a general phenomenon of chromatin proteins, as the *C. elegans* heterochromatin proteins HPL-1 and HPL-2 showed no significant changes in mobility. The signaling pathway(s) responsible for intestine-specific versus ubiquitous immobilization of BAF-1, which might include signaling via specific neurons (e.g., ASI neurons for dietary restriction; AFD neurons for heat shock; Bishop and Guarente, 2007; Prahlad *et al.*, 2008) are important questions for future work. Together these results show that BAF-1 immobilization at the nuclear lamina is a fundamental cellular response to stress. However, because dietary restriction and food deprivation are regulated by multiple pathways in *C. elegans* (Greer and Brunet, 2009), it will be interesting to investigate whether different dietary restriction regimes, as well as different stressors, lead to different patterns of BAF-1 immobilization.

Mechanisms of BAF-1 immobilization

Mass spectrometry analysis of GFP::BAF-1 from mixed-stage animal populations showed BAF-1 is phosphorylated on Ser-4, consistent with previous studies of human BAF (Bengtsson and Wilson, 2006; Nichols *et al.*, 2006) and *C. elegans* BAF-1 (Asencio *et al.*, 2012). We did not detect phosphorylation at two other sites reported in human BAF (Thr-2 and Thr-3 [Nichols *et al.*, 2006], equivalent to BAF-1 Ser-2 and Thr-3) that might be less abundant in *C. elegans* (Asencio *et al.*, 2012). BAF-1 Ser-4 phosphorylation appeared to increase in response to brief heat shock, but whether heat shock affects the localization or activity of its kinase (VRK-1) is unknown. Further analysis using S4A- or S4E-mutated BAF-1 strains, as well as *vrk-1* knockdown, confirmed that Ser-4 is important for BAF-1 dynamics. Interestingly, the mobility data of mutations in BAF-1 Ser-4 do not support a simple phosphorylation-immobilization model. This could be the result of altered protein–protein interactions in Ser-4 mutants

		$t_{1/2}$ (s)		Mobile (%)	
	Localization	Control	HS	Control	HS
BAF WT	NE	2.42 ± 0.12	2.01 ± 0.24	65 ± 1.6	44.2 ± 4.4
BAF S4A	NE+NP	2.21 ± 0.25	2.05 ± 0.11	38.7 ± 2	40.5 ± 5.9
BAF S4E	NE	2.67 ± 0.64	2.21 ± 0.24	45.4 ± 2.5	61.2 ± 2.6
BAF K6A	NE	2.57 ± 0.5	2.46 ± 0.47	60.5 ± 3	25.7 ± 1.64

HS, heat shock; NE, nuclear; NP, nucleoplasm; NE+NP, nuclear and mild nucleoplasm.

TABLE 1: Summary of the localization, $t_{1/2}$, and mobile/immobile fractions for each tested GFP::BAF-1 mutant strain in L1 larvae based on FRAP (± SEM).

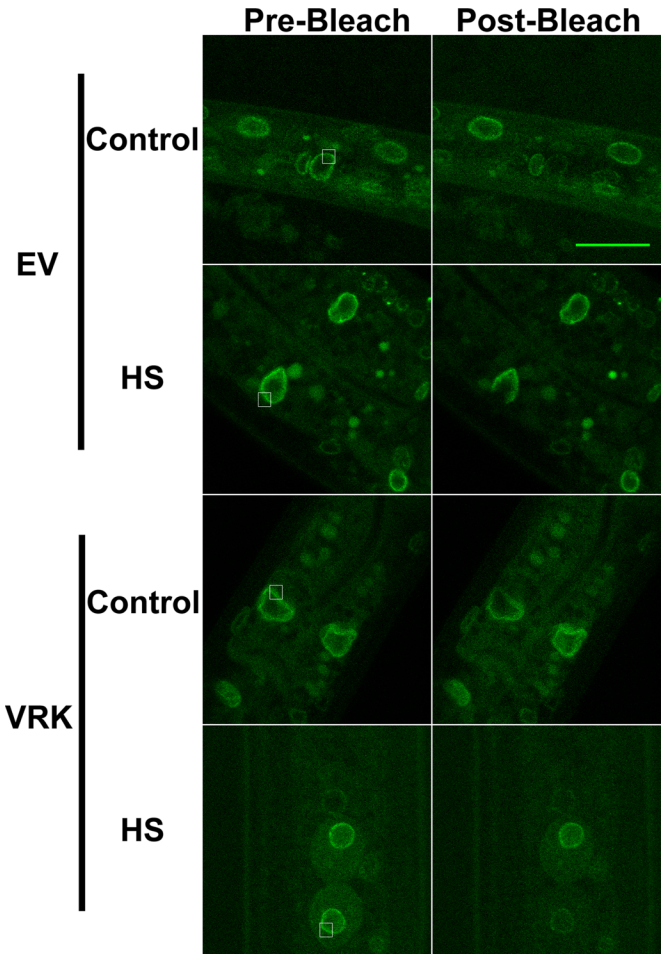

FIGURE 6: GFP::BAF-1 immobilization is regulated by *vrk-1*. FLIP analysis of GFP::BAF-1 in animals grown on empty vector (EV) or *vrk-1* RNAi (VRK) before and after heat shock (HS). Scale bar: 10 μm. Bleaching area: 3.1 μm^2.

due to imperfect mimicry of the phosphorylated state. Additionally, it is possible that other heat shock–dependent modifications, either on BAF-1 or on other proteins, regulate BAF-1 mobility.

GFP::BAF-1 immobilization is likely to be mediated by binding to a less mobile protein. We note that both emerin and lamin are immobile at the minute timescale (Figure 2G; Wiesel *et al.*, 2008). To understand the mechanisms of BAF-1 immobilization, we considered first the effects of BAF-1 mutations on its binding to partners in vitro and its localization and mobility in normal (unstressed) intestinal cells. This yielded novel insight, because BAF dynamics in nondividing cells were previously unstudied. The BAF-1 S4E mutation, which weakens DNA binding (Bradley *et al.*, 2005), also significantly (382-fold) reduced BAF-1 affinity for lamin, but showed normal affinity for emerin. This normal binding to emerin may explain why S4E-mutated GFP::BAF-1 localized normally in unstressed intestinal cells. The F46E mutant still localized at the nuclear lamina but was more nucleoplasmic in intestinal cells, suggesting a balance between eightfold weaker binding to lamin and 10-fold higher affinity for emerin. The S4A and K6A mutations, with two- to threefold weaker binding to lamin and two- to threefold stronger binding to emerin, localized normally. These results show that de facto biochemical defects (e.g., significantly reduced affinity for DNA and lamin) are compensated in nondividing cells by mechanism(s) that include increased affinity for emerin (and perhaps other LEM-domain proteins). The nuclear distribution of BAF-1 mutants might also be stabilized by additional factors, such as posttranslational modifications of emerin or other key partners. Indeed, human emerin binding to BAF is restricted to a specific chromatin- and lamin B–containing "niche," and is regulated by phosphorylation versus *O*-GlcNAcylation at a specific emerin residue (S173; Berk *et al.*, 2013).

BAF-1 immobilization as a fundamental cellular response to stress

BAF-1 is required for *C. elegans* embryos to survive exposure to ionizing radiation (Dittrich *et al.*, 2012); in this situation, it acts via the nuclease LEM-3, a conserved non–membrane-associated LEM-domain protein. Consistent with this role in surviving DNA damage, exposure of human cells to UV-induced damage causes BAF to interact with the damage-specific DNA-binding protein 2 and cullin 4E3 ubiquitin ligase (Montes de Oca *et al.*, 2009). Our work suggests that BAF-1 also responds dynamically to three other stresses: food deprivation, dietary restriction (*eat-2* mutation), and brief heat shock. Each stress has the potential to influence the localization, expression, or posttranslational modifications of proteins that bind BAF-1.

The BAF-1 mutants provided novel insight into BAF-1 immobility under normal (unstressed) conditions and in the case of heat shock. At 20°C, similar percentages (35–40%) of wild-type and K6A were immobile, suggesting immobility did not require binding to DNA or histones (both abolished by K6A; Segura-Totten *et al.*, 2002). Immobility was increased (from 35% in wild-type to 55–61%) by mutations that weakened binding to both DNA and lamin (S4A and S4E). Weaker binding cannot explain immobilization. However, for two mutations (K6A and S4A), higher immobile fractions in vivo correlated with higher affinity for emerin in vitro. The exception (S4E) had normal affinity but twofold slower rates of association and dissociation; thus bound S4E might tend to "linger" on emerin. About 55% of BAF-1 S4E was immobile under normal conditions, essentially the same as wild-type BAF-1 after heat shock (56% immobile). Overall BAF-1 immobility in intestinal cells correlated with normal or increased affinity for emerin in vitro.

Dietary restriction and insulin-like signaling regulate the *baf-1* gene: long-term effects on nuclear lamina function?

Both dietary restriction and short-term heat shock lead to transcriptional changes that can extend life span (Raynes *et al.*, 2012). We used chromatin immunoprecipitation data from the modENCODE database to analyze the promoter region of *baf-1*. We found that four transcription factors that modulate life span, either by dietary restriction or insulin-like signaling, namely SKN-1, PHA-4, DAF-16, and ELT-3; and other transcription factors (ALR-1, BLMP-1, LIN-15B) bind the *baf-1* promoter (see Figure S4). These data predict that stress signaling, in addition to immobilizing BAF-1 protein at the nuclear lamina, might also regulate BAF-1 protein levels. We speculate that this is a long-term effect, as we detected no significant change in GFP::BAF protein levels after overnight food deprivation (p value of 0.057, $n = 6$). Consistent with this idea, BAF-1 immobilization was only slightly reversed by feeding for 2 h.

Stress-induced BAF-1 immobilization and chromatin

Our most exciting and unexpected result is that caloric restriction and heat stress regulate BAF-1 dynamics in L1 larvae intestinal cells and stabilize BAF-1 localization at the nuclear lamina. To our knowledge, this is the first evidence that external stress can change the intranuclear mobility of any nuclear lamina protein. How might BAF-1 immobilization affect chromatin? A human BAF proteome

revealed 56 high-confidence targets in a single cell type, including multiple proteins that regulate histone modifications (Montes de Oca *et al.*, 2009). Because BAF both stabilizes nuclear lamina structure and influences histone posttranslational modifications (Montes de Oca *et al.*, 2011), stress-induced BAF-1 immobilization has the potential to stabilize chromatin structure and broadly influence gene expression.

MATERIALS AND METHODS

C. elegans strains

C. elegans strains were handled as described previously (Brenner, 1974). Strains N2 (wild-type), DP38 *unc-119*(*ed3*), and *eat-2*(*ad1116*) were obtained from the Caenorhabditis Genetics Center (University of Minnesota, Minneapolis, MN). Strains HPL-1::GFP and FR463 (HPL-2::GFP+pRF4) were kindly provided by F. Palladino (CNRS). The independent GFP::BAF-1–expressing strains (YG1001, YG2501, YG2502), GFP::BAF-1 S4A (YG2503, YG2504), GFP::BAF-1 S4E (YG2505, YG2506), GFP::BAF-1 K6A (YG2507, YG2508), GFP::BAF-1 F46E (YG2511, YG2512), and the independent emerin::GFP–expressing strain (YG002) were generated by microparticle bombardment of DP38 animals, as described previously (Margalit *et al.*, 2007b), and were outcrossed three times. *eat-2*(*ad1116*); GFP::BAF-1(YG1001) was generated by crossing these two stains.

Dietary restriction, food deprivation, and heat shock conditions

L1 measurements were performed by synchronizing embryos as previously described (Motohashi *et al.*, 2006). Control and *eat-2* embryos were seeded on OP50 *Escherichia coli* plates overnight at 23°C, while empty plates were used for food deprivation experiments. For heat shock, plates were incubated for 1 h at 37°C.

Bacterial expression of the mutant MBP::BAF-1 proteins

Wild-type *baf-1* gene and all mutated *baf-1* cDNAs were cloned into the pMal C2 vector containing maltose-binding protein (MBP) parallel 1 (New England Biolabs). In this construct *baf-1* is located 5′ to the multiple cloning site of the pMAL plasmid. Plasmids were transformed into *E. coli* BL21(DE3)-(codon plus-RIL), and expressed proteins were purified on amylose resin per the manufacturer's protocol (New England Biolabs; www.neb.com/products/e8021-amylose-resin). Recombinant His-tagged Ce-lamin-tail, Ce-lamin R55H, and Ce-emerin residues 1–125 were purified as previously described (Ben-Harush *et al.*, 2009), dialyzed into column buffer (20 mM sodium phosphate buffer, 200 mM NaCl, 1 mM EDTA) for 24 h at 4°C, and then filtered by centrifugation (Nanosep MF 0.2 μm; Pall Life Sciences). Protein concentration was measured with NanoDrop ND-100 (NanoDrop, Wilmington, DE).

Image analysis, microscopy, and live-cell imaging

Live fluorescence images were acquired with the Leica SP5 confocal microscope and a 63×/1.4 oil-immersion objective. Imaging was performed and initially analyzed with Leica Application Suite 2.3.1. Bleaching was done on a single *z*-plane, at 100% transmission. Imaging typically required 1–6% of laser power. For pre- and post-bleach images, four frames were extracted and averaged from corresponding movies using ImageJ. Graphs were generated from multiple regions of interest after normalization and averaging. Worms were mounted on agarose pads and paralyzed with 1–10 mM levamisole and immediately taken for imaging. Typically, animals were imaged for 5–30 min after levamisole admission. When visible, the FLIP experiments started with the most anterior intestinal cells, and we moved backward in sequential FLIPs. For FRAP analysis, all strains were imaged with a Leica SP5 confocal microscope and a 63×/1.4 oil-immersion objective. GFP::BAF-1 fluorescence was photobleached by a 488-nm laser in a defined region of each cell and was imaged with a 488-nm (Figure 1) or 496-nm laser for all other experiments. For FRAP analysis, fluorescence intensity in the bleached area, the background area, and the total cell area were measured as a function of time after bleaching and were normalized essentially as described previously (Rabut and Ellenberg, 2005). For FLIP experiments, we used 488-nm light to repetitively bleach GFP::BAF-1 in a region of interest. For determination of the half-time of FRAP, the normalized fluorescence intensity of the mobile fraction was divided by two. The corresponding time (half-time) was extracted from the plot/equation (Rabut and Ellenberg, 2005).

Protein distribution

Protein distribution was calculated using ImageJ (Schneider *et al.*, 2012) by measuring the fluorescence intensity along a line crossing the nucleus. For each graph, five to seven nuclei were normalized and averaged by aligning peaks representing the nuclear envelope. Error bars represent SEM. *p* values were calculated by averaging the intensity of seven adjacent dots along the crossing line. Averages of measured nuclei from different BAF mutations were compared with wild type using a two-tailed *t* test.

GFP-TRAP-M

For isolation of GFP::BAF-1 protein, YG1001 asynchronous population worms were grown in 9-cm plates. Six plates were subjected to heat shock (37°C, 1 h). Worms were collected, washed twice with M9, and resuspended in 200 ml lysis buffer (10 mM Tris-HCl, pH 7.5, 150 mM NaCl, 0.5 mM EDTA, 0.5% NP40, 1X Protease Inhibitor Cocktail [Roche, Indianapolis, IN]). Lysates were frozen in liquid nitrogen and thawed on ice 30 min, with extensive pipetting every 10 min. Samples were then sonicated (30 s, five times) and centrifuged (20,000 × *g*, 10 min, 4°C). GFP::BAF-1 was purified using GFP-Trap antibodies per the manufacturer's protocol (GFP-TRAP_M; ChromoTek). Samples were boiled (100°C, 10 min), resolved by SDS–PAGE (15% acrylamide), and stained with Coomassie blue. GFP::BAF-1 bands were identified by immunoblotting an additional lane with mouse-anti GFP (1:1000; Roche) and excised for MS analysis.

In-gel proteolysis and mass spectrometry analysis

Proteins in excised gel bands were reduced (3 mM dithiothreitol), modified (12 mM iodoacetamide), and digested with modified trypsin (Promega, Madison, WI) at a 1:10 enzyme-to-substrate ratio in 10 mm ammonium bicarbonate and 10% acetonitrile. Tryptic peptides were resolved by reverse-phase chromatography on 0.075 × 200–mm fused silica capillaries (J&W; Agilent, Santa Clara, CA) packed with Reprosil reversed-phase material (Dr. Maisch GmbH, Ammerbuch-Entringen, Germany). The peptides were eluted for 65 min using a linear 5–45% gradient followed by 15 min in 95% acetonitrile/0.1% formic acid [vol/vol] in water at flow rates of 0.25 μl/min. Mass spectrometry was performed with an ion-trap mass spectrometer (OrbitrapXL; Thermo-Finnigan, San Jose, CA) in a positive mode using repetitively full MS scan followed by collision-induced dissociation of the seven most-dominant ions selected from the first MS scan. Multistage activation was used to analyze phosphopeptides. The mass spectrometry data were analyzed using Sequest 3.31 software, searching against the uniprot database and against a specific sequence with 5 ppm accuracy.

BIAcore analysis

Binding was analyzed using a BIAcore 3000 (BIAcore, Uppsala, Sweden) and sensor chip CM5 (BIAcore), at 25°C. The chip was activated using the BIAcore EDC/NHS amine-coupling protocol (www.biacore.com). In kinetics experiments, recombinant His::lamin R55H and His::emerin 1–125 proteins at 10 µg/ml in 10 mM acetate (pH 4) were immobilized and gave ~2000 resonance units (RU) and 1200 RU, respectively. Analytes were injected at 30 µl/min in 10 mM phosphate (pH 7.4), 150 mM NaCl, and 0.005% Tween 20. The chip was regenerated using 10 mM phosphate (pH 7.4), 150 mM NaCl, and 0.005% Tween 20. Results were evaluated using BIAevaluation software version 4.1. The 1.1 Langmuir model was used to fit experimental results and calculate affinities and kinetics constants.

ACKNOWLEDGMENTS

We thank Tsafi Danieli for helping with protein expression and the Smoler Proteomics Center (Technion) for mass spectrometry analyses. We also thank Francesca Palladino for providing the strains expressing GFP-fused HPL-1 and HPL-2 and Alon Zaslaver for critical reading of the manuscript. We gratefully acknowledge funding from Morasha Legacy 1798/10, the Binational Israel-USA Science Foundation, the National Institutes of Health (RO1 GM048646 to K.L.W. and Y.G.), the Israel Ministry of Health (MOH 2965), the Muscular Dystrophy Association, and the COST NANONET (BM1002).

REFERENCES

Asencio C, Davidson IF, Santarella-Mellwig R, Ly-Hartig TB, Mall M, Wallenfang MR, Mattaj IW, Gorjánácz M (2012). Coordination of kinase and phosphatase activities by Lem4 enables nuclear envelope reassembly during mitosis. Cell 150, 122–135.

Bengtsson L, Wilson KL (2006). BAF phosphorylation on Ser-4 regulates emerin binding to lamin A in vitro and emerin localization in vivo. Mol Biol Cell 17, 1154–1163.

Ben-Harush K, Wiesel N, Frenkiel-Krispin D, Moeller D, Soreq E, Aebi U, Herrmann H, Gruenbaum Y, Medalia O (2009). The supramolecular organization of the *C. elegans* nuclear lamin filament. J Mol Biol 386, 1392–1402.

Berk JM, Maitra S, Dawdy AW, Shabanowitz J, Hunt DF, Wilson KL (2013). O-Linked β-N-acetylglucosamine (O-GlcNAc) regulates emerin binding to barrier to autointegration factor (BAF) in a chromatin- and lamin B-enriched "niche." J Biol Chem 288, 30192–30209.

Bishop NA, Guarente L (2007). Genetic links between diet and lifespan: shared mechanisms from yeast to humans. Nat Rev Genet 8, 835–844.

Bradley CM, Ronning DR, Ghirlando R, Craigie R, Dyda F (2005). Structural basis for DNA bridging by barrier-to-autointegration factor. Nat Struct Mol Biol 12, 935–936.

Brenner S (1974). The genetics of *Caenorhabditis elegans*. Genetics 77, 71–94.

Broers JL, Kuijpers HJ, Ostlund C, Worman HJ, Endert J, Ramaekers FC (2005). Both lamin A and lamin C mutations cause lamina instability as well as loss of internal nuclear lamin organization. Exp Cell Res 304, 582–592.

Cai M, Huang Y, Ghirlando R, Wilson KL, Craigie R, Clore GM (2001). Solution structure of the constant region of nuclear envelope protein LAP2 reveals two LEM-domain structures: one binds BAF and the other binds DNA. EMBO J 20, 4399–4407.

Cai M, Huang Y, Suh JY, Louis JM, Ghirlando R, Craigie R, Clore GM (2007). Solution NMR structure of the barrier-to-autointegration factor-emerin complex. J Biol Chem 282, 14525–14535.

Cai M, Huang Y, Zheng R, Wei SQ, Ghirlando R, Lee MS, Craigie R, Gronenborn AM, Clore GM (1998). Solution structure of the cellular factor BAF responsible for protecting retroviral DNA from autointegration. Nat Struct Biol 5, 903–909.

Capanni C, Cenni V, Haraguchi T, Squarzoni S, Schüchner S, Ogris E, Novelli G, Maraldi N, Lattanzi G (2010). Lamin A precursor induces barrier-to-autointegration factor nuclear localization. Cell Cycle 9, 2600–2610.

Chen H, Engelman A (1998). The barrier-to-autointegration protein is a host factor for HIV type 1 integration. Proc Natl Acad Sci USA 95, 15270–15274.

Dechat T, Gajewski A, Korbei B, Gerlich D, Daigle N, Haraguchi T, Furukawa K, Ellenberg J, Foisner R (2004). LAP2a transiently localizes to telomeres and to defined chromatin regions during nuclear assembly. J Cell Sci 117, 6117–6128.

Dittrich CM, Kratz K, Sendoel A, Gruenbaum Y, Jiricny J, Hengartner MO (2012). LEM-3—a LEM domain containing nuclease involved in the DNA damage response in *C. elegans*. PLoS One 7, e24555.

Furukawa K (1999). LAP2 binding protein 1 (L2BP1/BAF) is a candidate mediator of LAP2- chromatin interaction. J Cell Sci 112, 2485–2492.

Furukawa K, Sugiyama S, Osouda S, Goto H, Inagaki M, Horigome T, Omata S, McConnell M, Fisher PA, Nishida Y (2003). Barrier-to-autointegration factor plays crucial roles in cell cycle progression and nuclear organization in *Drosophila*. J Cell Sci 116, 3811–3823.

Gorjánácz M, Klerkx EPF, Galy V, Santarella R, López-Iglesias C, Askjaer P, Mattaj IW (2007). C. elegans BAF-1 and its kinase VRK-1 participate directly in postmitotic nuclear envelope assembly. EMBO J 26, 132–143.

Greer EL, Brunet A (2009). Different dietary restriction regimens extend lifespan by both independent and overlapping genetic pathways in *C. elegans*. Aging Cell 8, 113–127.

Haraguchi T, Koujin T, Osakada H, Kojidani T, Mori C, Masuda H, Y H (2007). Nuclear localization of barrier-to-autointegration factor is correlated with progression of S phase in human cells. J Cell Sci 120, 1967–1977.

Harris D, Engelman A (2000). Both the structure and DNA binding function of the barrier-to-autointegration factor contribute to reconstitution of HIV type 1 integration in vitro. J Biol Chem 275, 39671–39677.

Holaska JM, Lee KK, Kowalski AK, Wilson KL (2003). Transcriptional repressor germ cell-less (GCL) and barrier-to-autointegration factor (BAF) compete for binding to emerin in vitro. J Biol Chem 278, 6969–6975.

Huang Y, Cai M, Clore GM, Craigie R (2011). No interaction of barrier-to-autointegration factor (BAF) with HIV-1 MA, cone-rod homeobox (Crx) or MAN1-C in absence of DNA. PLoS One 6, e25123.

Jacque JM, Stevenson M (2006). The inner-nuclear-envelope protein emerin regulates HIV-1 infectivity. Nature 441, 581–582.

Johnson TE, Mitchell DH, Kline S, Kemal R, Foy J (1984). Arresting development arrests aging in the nematode *Caenorhabditis elegans*. Mech Ageing Dev 28, 23–40.

Lee KK, Haraguchi T, Lee RS, Koujin T, Hiraoka Y, Wilson KL (2001). Distinct functional domains in emerin bind lamin A and DNA-bridging protein BAF. J Cell Sci 114, 4567–4573.

Lin CW, Engelman A (2003). The barrier-to-autointegration factor is a component of functional human immunodeficiency virus type 1 preintegration complexes. J Virol 77, 5030–5036.

Liu J, Lee KK, Segura-Totten M, Neufeld E, Wilson KL, Gruenbaum Y (2003). MAN1 and emerin have overlapping function(s) essential for chromosome segregation and cell division in *C. elegans*. Proc Natl Acad Sci USA 100, 4598–4603.

Margalit A, Brachner A, Gotzmann J, Foisner R, Y G (2007a). Barrier-to-autointegration factor —a BAFfling little protein. Trends Cell Biol 17, 202–208.

Margalit A, Liu J, Fridkin A, Wilson KL, Gruenbaum Y (2005a). A lamin-dependent pathway that regulates nuclear organization, cell cycle progression and germ cell development. Novartis Found Symp 264, 231–240.

Margalit A, Neufeld E, Feinstein N, Wilson KL, Podbilewicz B, Gruenbaum Y (2007b). Barrier-to-autointegration factor (BAF) is required for blocking premature cell fusion, vulva formation, germ cell development and survival, DTC migration and adult muscle integrity in *C. elegans*. J Cell Biol 178, 661–673.

Margalit A, Segura-Totten M, Gruenbaum Y, Wilson KL (2005b). Barrier-to-autointegration factor is required to segregate and enclose chromosomes within the nuclear envelope and assemble the nuclear lamina. Proc Natl Acad Sci USA 102, 3290–3295.

Mastick GS, McKay R, Oligino T, Donovan K, Lopez AJ (1995). Identification of target genes regulated by homeotic proteins in *Drosophila melanogaster* through genetic selection of Ultrabithorax protein-binding sites in yeast. Genetics 139, 349–363.

Moir RD, Spann TP, Lopez-Soler RI, Yoon M, Goldman AE, Khuon S, Goldman RD (2000). The dynamics of the nuclear lamins during the cell cycle—relationship between structure and function. J Struct Biol 129, 324–334.

Montes de Oca R, Andreassen PR, Wilson KL (2011). Barrier-to-autointegration factor influences specific histone modifications. Nucleus 2, 580–590.

Montes de Oca R, Shoemaker CJ, Gucek M, Cole RN, Wilson KL (2009). Barrier-to-autointegration factor proteome reveals chromatin-regulatory partners. PLoS One 4, e7050.

Montes de Oca RM, Lee KK, Wilson KL (2005). Binding of barrier to autointegration factor (BAF) to histone H3 and selected linker histones including H1.1. J Biol Chem 280, 42252–42262.
Motohashi T, Tabara H, Kohara Y (2006). Protocols for large scale in situ hybridization on *C. elegans* larvae. WormBook 1–8.
Nichols RJ, Wiebe MS, Traktman P (2006). The vaccinia-related kinases phosphorylate the N-terminus of BAF, regulating its interaction with DNA and its retention in the nucleus. Mol Biol Cell 17, 2451–2464.
Olsen A, Vantipalli MC, Lithgow GJ (2006). Lifespan extension of *Caenorhabditis elegans* following repeated mild hormetic heat treatments. Biogerontology 7, 221–230.
Palgunow D, Klapper M, Döring F (2012). Dietary restriction during development enlarges intestinal and hypodermal lipid droplets in *Caenorhabditis elegans*. PLoS One 7, e46198.
Prahlad V, Cornelius T, Morimoto RI (2008). Regulation of the cellular heat shock response in *Caenorhabditis elegans* by thermosensory neurons. Science 320, 811–814.
Puente XS *et al.* (2011). Exome sequencing and functional analysis identifies BANF1 mutation as the cause of a hereditary progeroid syndrome. Am J Hum Genet 88, 650–656.
Rabut G, Ellenberg J (2005). Photobleaching Techniques to Study Mobility and Molecular Dynamics of Proteins in Live Cells: FRAP, iFRAP and FLIP, Cold Spring Harbor, NY: Cold Spring Harbor Laboratory Press.
Raynes R, Leckey BDJ, Nguyen K, Westerheide SD (2012). Heat shock and caloric restriction have a synergistic effect on the heat shock response in a sir2.1-dependent manner in *Caenorhabditis elegans*. J Biol Chem 287, 29045–29053.
Rothbauer U, Zolghadr K, Muyldermans S, Schepers A, Cardoso MC, Leonhardt H (2008). A versatile nanotrap for biochemical and functional studies with fluorescent fusion proteins. Mol Cell Proteomics 7, 282–289.
Schneider CA, Rasband WS, Eliceiri KW (2012). NIH Image to ImageJ: 25 years of image analysis. Nat Methods 9, 671–675.
Schott S, Coustham V, Simonet T, Bedet C, Palladino F (2006). Unique and redundant functions of C. elegans HP1 proteins in post-embryonic development. Dev Biol 298, 176–187.
Schutz W, Alsheimer M, Ollinger R, Benavente R (2005). Nuclear envelope remodeling during mouse spermiogenesis: postmeiotic expression and redistribution of germline lamin B3. Exp Cell Res 307, 285–291.
Segura-Totten M, Kowalski AK, Craigie R, Wilson KL (2002). Barrier-to-autointegration factor: major roles in chromatin decondensation and nuclear assembly. J Cell Biol 158, 475–485.
Shimi T, Koujin T, Segura-Totten M, Wilson KL, Haraguchi T, Hiraoka Y (2004). Dynamic interaction between BAF and emerin revealed by FRAP, FLIP, and FRET analyses in living HeLa cells. J Struct Biol 147, 31–41.
Shumaker DK, Lee KK, Tanhehco YC, Craigie R, Wilson KL (2001). LAP2 binds to BAF-DNA complexes: requirement for the LEM domain and modulation by variable regions. EMBO J 20, 1754–1764.
Shun MC, Daigle JE, Vandegraaff N, Engelman A (2007). Wild-type levels of human immunodeficiency virus type 1 infectivity in the absence of cellular emerin protein. J Virol 81, 166–172.
Simon DN, Wilson KL (2011). The nucleoskeleton as a genome-associated dynamic "network of networks." Nat Rev Mol Cell Biol 12, 695–708.
Skoko D *et al.* (2009). Barrier-to-autointegration factor (BAF) condenses DNA by looping. Proc Natl Acad Sci USA 106, 16610–16615.
Van Maele B, Busschots K, Vandekerckhove L, Christ F, Debyser Z (2006). Cellular co-factors of HIV-1 integration. Trends Biochem Sci 31, 98–105.
Wagner N, Krohne G (2007). LEM-domain proteins: new insights into lamin-interacting proteins. Int Rev Cyt 261, 1–46.
Walker G, Houthoofd K, Vanfleteren JR, Gems D (2005). Dietary restriction in *C. elegans*: from rate-of-living effects to nutrient sensing pathways. Mech Aging Dev 126, 929–937.
Wang X *et al.* (2002). Barrier to autointegration factor interacts with the cone-rod homeobox and represses its transactivation function. J Biol Chem 277, 43288–43300.
Wiesel N, Mattout A, Melcer S, Melamed-Book N, Herrmann H, Medalia O, Aebi U, Gruenbaum Y (2008). Laminopathic mutations interfere with the assembly, localization and dynamics of nuclear lamins. Proc Natl Acad Sci USA 105, 180–185.
Zheng R, Ghirlando R, Lee MS, Mizuuchi K, Krause M, Craigie R (2000). Barrier-to-autointegration factor (BAF) bridges DNA in a discrete, higher-order nucleoprotein complex. Proc Natl Acad Sci USA 97, 8997–9002.